Journal of Engineering Science 15(1), 2024, 45-57
DOI: https://doi.org/10.3329/jes.v15i1.76032

JES
an international Journal

CHITOSAN BASED ZINC AND COPPER NANOPARTICLES: SYNTHESIS, CHARACTERIZATION AND ANTIBACTERIAL ACTIVITY INVESTIGATION

Gazi Jahirul Islam[1*], Shaheda Zannah[2] and Md. Mohinuddin[1]

[1]*Department of Chemistry, University of Barishal, Barishal-8254, Bangladesh*
[2]*Department of Pharmacy, Southeast University, Dhaka-1208, Bangladesh*

Received: 27 April 2024 Accepted: 30 May 2024

ABSTRACT

Chitosan biopolymer has been used as a key supporting material for the synthesis of metallic nanoparticles (MNPs) due to its exceptional qualities, which include good capping and stabilizing capabilities, biocompatibility, biodegradability, eco-friendliness, polycationic and non-toxicity. In this study, chitosan-based metal nanoparticles, such as copper nanoparticles (Chi-Cu NPs) and zinc nanoparticles (Chi-Zn NPs) have been synthesized, characterized and checked for their bacteriological properties. The solution casting method has been employed to produce metal nanoparticles based on chitosan. FTIR, TGA, and SEM analysis were employed to characterize the produced nanoparticles. The produced materials are nanomaterials with a size range of 1-100 nm, as demonstrated by the SEM photograph. The generated nanoparticles showed increased antimicrobial activity. Chi-Zn NPs have zones of inhibition of 38, 31, 30 and 39 and Chi-Cu NPs have zones of inhibition of 32, 36, 37 and 32 mm against Pseudomonas aeruginosa, Salmonella bovismorbificans, Salmonella typhi and Escherichia coli bacteria, respectively. Whereas the standard medication kanamycin have zones of inhibition 22, 22, 20 and 20 against those bacteria, respectively.

Kew Words: Chitosan, copper nanoparticle (Chi-Cu NPs), Zinc nanoparticle (Chi-Zn NPs), antibacterial activity

1. INTRODUCTION

Over the past decade, we have seen a sharp rise in interest in the natural polymers, which includes chitin, cellulose, and starch, because they used for variety of purposes, including energy storage, transportation, signaling, and structural components (Ates et al., 2020; Torres et al., 2019). The deacetylated form of chitin, chitosan, is a simple polysaccharide that can be made from the shells of shrimp, prawns, and crabs. In order to establish a physiologically inert and flexible environment for sensing and manipulating macromolecules and microbes in devices, chitosan exhibits biocompatibility and biodegradability (Khan & Alamry, 2021). The utilization of chitosan and its derivatives as materials for wastewater treatment, biosensors, actuators, artificial muscles, environmentally sensitive membranes, electrolytes, and other components in high-energy batteries has been the subject of active research recently (Banitaba et al., 2022; Karki et al., 2021).

Multidrug-resistant (MDR) bacteria are becoming more prevalent, and this poses a serious risk to public health (Tanwar et al., 2014). MDR bacteria like Klebsiella pneumonia, Escherichia coli, Streptococcus pneumonia, Enterococcus faecalis, and Staphylococcus aureus can now be found in our surroundings and are not limited to medical situations (Vivas et al., 2019). By 2050, the true cost of antibiotic resistance is expected to be 300 million to avoided deaths (O'neill, 2014). Metal NPs have garnered considerable attention as an antimicrobial agent because of their high surface area to volume ratio (Ye et al., 2022).

The first description of chitosan nanoparticles dates back to 1994 when Ohya and coworkers (Ohya et al., 1994) suggested using emulsified and cross-linked chitosan nanoparticles to deliver the anticancer medication 5-fluorouracil intravenously. Since then, these systems have been the subject of in-depth research for the administration of drugs. Furthermore, numerous researchers have designed novel chitosan nanoparticle formulations with other matrix-forming components (Detsi et al., 2020). The techniques include ionic gelation (Ahmed et al., 2023), polyelectrolyte complexation (Lefnaoui et al., 2018), emulsion-droplet coalescence (Rosales-Martínez et al., 2018), reverse micellar approach (Victor et al., 2013), and de-solvation (Benchasattabuse, 2015). These techniques are all examples of bottom-up fabrication processes (Chan & Kwok, 2011), where molecules are assembled in solution to form specific structures as nanoparticles. Bottom-up technologies' delivery systems typically exhibit size polydispersity (Verma et al., 2009), which occasionally restricts the utility of nanoparticles.

*Corresponding Author: gjahir@yahoo.com
ISSN 2075-4914 (print); ISSN 2706-6835 (online)

Zinc oxide (ZnO) nanoparticles are one of the most studied nanoparticles in both fundamental research and practical applications, such as solar energy conversion, photocatalysis, varistors, electrostatic dissipative coating, luminescence, chemical sensors, and transparent UV protection films. ZnO nanoparticles have previously been produced using a variety of methods, such as spray pyrolysis (Wallace et al., 2013), hydrothermal synthesis (Gerbreders et al., 2020), precipitation (Raoufi, 2013), and sol-gel approach (Ba-Abbad et al., 2013). Because of its amine and hydroxyl groups, chitosan has the remarkable ability to form metal complexes with zinc metal (Wang et al., 2004). As a result, the chitosan-ZnO combination has generated a lot of interest due to its possible use as a medication and UV protector. On the other hand, Cu-NPs are becoming more and more popular due to their advantageous qualities (thermal and electrical conductivity), which can be obtained for a lot less money than other noble metals like gold and silver (Tito et al., 2021). Cu is known to be non-toxic to animals and to possess antibacterial and antifungal properties (Ahmed et al., 2021; Zangeneh et al., 2019). Cu NPs produced in the sepiolite matrix, for instance, have been shown to have bactericidal characteristics by Esteban-Cubillo and coworkers (Esteban-Cubillo et al., 2006). Furthermore, antifungal and antifouling characteristics of a Cu NP-polymer composite have been reported by Cioffi et al. 2005 (Cioffi et al., 2005). Some techniques, including thermal reduction (Salavati-Niasari & Davar, 2009), sonochemical reduction (Bhosale & Bhanage, 2016), chemical reduction (Khan et al., 2016), vacuum vapor deposition (Khan et al., 2021), micro-emulsion technique (Qiu et al., 1999), and laser ablation (Al-Jumaili et al., 2018) have been developed for the synthesis of Cu NPs. It's interesting to note that the majority of these techniques use an oxygen-free environment during synthesis because atmospheric oxygen quickly oxidizes the precursor Cu NPs (Park et al., 2007; Soomro et al., 2014). All of these methods are not free from restrain which is why furthermore development is required.

Natural and linear biopolyamino-saccharide chitosan has drawn a lot of interest as a functional biopolymer with uses in food, medicine, cosmetics, and pharmaceuticals . One of the primary sources of chitosan biopolymer is shrimp shells, which were utilized in this research as the raw material for chitosan manufacturing, and the resulting chitosan is then employed to manufacture metal nanoparticles based on chitosan. As was covered in previous sections, the synthesis and characterization of chitosan nanoparticles would be crucial and have numerous uses in a variety of commercial and medical contexts.

2. EXPERIMENTAL

2.1 Materials and Methods

2.1.1 Instruments

Electric balance (AND-HR-200), Electric oven (YCO-010 Series), IR (IR Prestige-21, Shimadzu), Furnace (Thermo Scientific Thermolyne, FB1415M), Sonicator (POWER SONIC 603), Scanning electron microscopy (SEM) (JEOL JSM-6490LA), Thermal gravimetric analysis (TGA-50, Shimadzu)

2.1.2 Raw Materials, Chemicals, and Reagents

Shrimp shell**,** Hydrochloric acid (E-Merck, Germany)**,** Acetic acid**,** Zinc oxide**,** Copper (ll) sulphate pentahydrate**,** Hydrazine hydrate solution**,** Sodium hydroxide, (E-Merck, Germany)

2.2 Preparation of Chitosan

Shrimp shells were collected from local market. Shells were washed with water for several times and the sun-dried for few days until they were dry. The dry shell was pulverized into coarse particles using a centrifugal grinding mill to produce a product with a uniform size. Before usage, the dried ground shells were kept at room temperature in opaque plastic bottles. The improved process was used to produce chitosan from the waste of shrimp shells.

2.2.1 Steps of methods

This process mainly involved the following steps.

2.2.1.1Demineralization of shells

Demineralization is the process of substituting hydroxide (OH^-) ions and hydrogen ions (H^+). The method used in modern industrial water softening is called demineralization. The shells were suspended at room temperature in a 1:12 (W/V) ratio containing 7% HCl during this phase. The shells were thoroughly squashed after 45 hours and were washed with water to remove the calcium chloride and acid.

2.2.1.2 Deproteinization of shells

The process of deproteinization involves either hydrolyzing or precipitating proteins out of a solution to remove them from a biological sample. The demineralized shells were treated with 7% NaOH at 80℃ for 26 hours, with a solid to solvent ratio of 1:12 (W/V), to extract protein from the material. After that, the residue was gathered and run under the tap until it became neutral and then sun-dried which gave the resultant product chitin.

2.2.1.3 The preparation of Chitosan by deacetylation of chitin

Removal of acetyl groups from the chitin was achieved by using 70% NaOH solution with solid to solvent ratio of 1:12 (W/V) at room temperature for 74 hours. The reaction mechanism is shown in Figure 1. To ensure a uniform reaction, the mixture was frequently agitated. After that, the chitosan was rinsed with distilled water and cleaned under running tap water, after which it was filtered and oven-dried. Thus, white to off-white flakes of chitosan were produced.

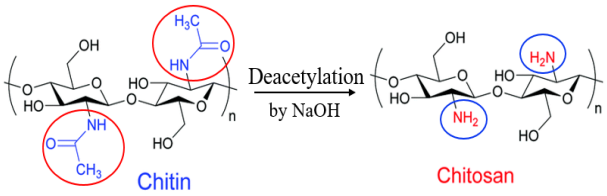

Figure 1: Conversion of Chitin to Chitosan by deacetylation process

2.3 Method for the preparation of Chitosan-Zn NPs

0.3g ZnO powder was dissolved in 80 mL of 1% acetic acid where it changed to zinc cations. 1 gram of chitosan was dissolved in 100 mL 1% acetic acid. After mixing 20 mL of ZnO solution and 20 mL of chitosan solution, the mixture was sonicated for 10 minutes. Then the solution was heated to a temperature of between 50-80 ℃ in a water bath with magnetic stirring for about an hour. The mixture was then progressively combined with 1M NaOH until the NPs were completely produced. NaOH accelerates the reduction rate of Zn^{2+} to Zn^{0} and as well as nucleation rate thereby increasing the rate of formation of the Chitosan-Zn NPs. It was then filtered, cleansed with distilled water for many times, and dried. In this instance, we added NaOH after the heat, and as soon as we added even a small quantity of NaOH, the production of NPs began and finished more quickly. This strategy differs from the others that are currently in use (AbdElhady, 2012; Wang & Muhammed, 1999).

2.4 Method for the preparation of Chitosan-Cu metal NPs

The methods described in Mallick S. et al. 2012 (Mallick et al., 2012) are followed in this preparation. In this experiment, 1.0 g of chitosan was dissolved in 100 mL of 1% acetic acid solution and 1.0 g of chitosan was dissolved in 100 mL 1% acetic acid solution. A light blue solution was obtained by mixing 50 mL of both solutions, which was sonicating for 10 minutes, and then transferred the solution to a 250 mL round-bottom flask. The flask was then placed in an oil bath with vigorous stirring and refluxed for 20 minutes at a temperature of about 100 °C. After adding roughly 1.0 mL of a 0.6 M NaOH solution, the solution's turned blue lightened to brown. Following roughly 20 minutes, the aforementioned solution was constantly stirred while nearly 1.0 mL of hydrazine hydrate solution was added. The mixture started as yellow and eventually turned reddish brown after nearly 30 minutes hitting. An extra ten to twenty minutes were given to the reaction to continue. After being removed from the oil bath, the flask was allowed to cool to room temperature. To get rid of hydrazine, the solution and precipitate were pellet washed multiple times with distilled water after centrifuging at 5300 rpm.

2.5 Moisture Content

Using the gravimetric approach, the produced chitosan's moisture content was ascertained. After being weighed out at 2.0 g, the chitosan was baked for 40 minutes at 102℃. After that, it was allowed to cool to room temperature for ten minutes in a desiccator. It was immediately weighted, and the following method was used to determine the percentage of moisture content.

$$\% \text{ of moisture content} = \frac{(\text{Wet weight,g} - \text{dry weight,g}) \times 100}{\text{Wet weight,g}} \quad (1)$$

2.6 Ash Content

2.0 g of chitosan sample was added to a crucible that had previously been lit, cooled, and tarred to calculate the ash value of the material. The samples were heated for 4 hours at 650 ℃ in a muffle furnace. After being allowed to cool to a temperature of less than 200 ℃ in the furnace, the crucibles were put into desiccators that had a vented top.

$$\% \text{ of Ash content} = \frac{(\text{Weight of residue,g}) \times 100}{\text{Sample weight,g}} \quad (2)$$

2.7 Solubility Test

Solubility of chitosan was observed in different types of mineral acids, organic acids, and other types of chemical solvents.

2.8 FTIR Test

Infrared spectra were recorded on an FTIR spectrophotometer (IR Prestige-21, Shimadzu) in the region 4500-400 cm^{-1} using KBr pellets.

2.9 Scanning electron microscopy of the Nanoparticles

Surface analysis of the produced NPs were performed using a Carl Zeiss Scanning Electron Microscope (Germany). A fine film was obtained by drying the NP suspension in a desiccator for at least 24 hours after 10 µl of the diluted suspension was applied to an aluminum stub. Under an extremely high vacuum, a gold layer was sputter-coated onto the NP film that had developed. Using smart SEM software, EVO 18 microscopes were used to take SEM images.

2.10 Antibacterial Activity

The antibacterial activity of the complexes was tested against Gram-negative *Pseudomonas aeruginosa*, Gram-negative *Salmonella bovismorbificans*, Gram-negative *Salmonella typhi*, and Gram-negative *Escherichia coli*. The disc diffusion approach was used to carry out the activities (Borges et al., 2013; Corbalán et al., 2021). Each disc was put on plates that had been infected with bacteria and contained 30 µg of chemical. The results of the growth inhibition were contrasted with those of Kanamycin, a common antibiotic.

3. RESULTS AND DISCUSSION

3.1 Moisture content

The results of the physio-chemical and functional properties of the prepared chitosan are given in Table 1. The prepared chitosan from shrimp shell was compared with the extra pure one. Usually, chitosan from shrimp shells contains moisture in the range of 1.00-1.30% depending on the season, relative humidity, and intensity of sunlight. It has been found that the moisture content of prepared chitosan is 1.25% while that for purchased extra pure is 1.24% (Figure 2) and has a good agreement.

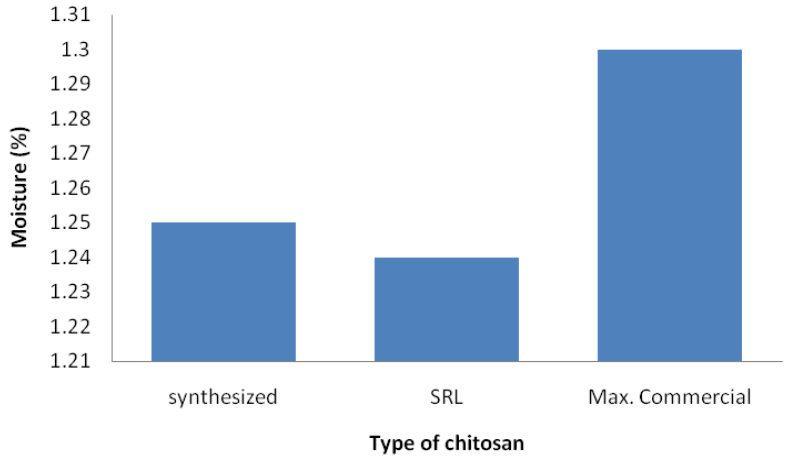

Figure 2: Moisture content of the chitosan

3.2 Ash content

Ash content exhibits the effectiveness of the demineralization step in removing minerals. From Table 1 shown that the ash content for the synthesized and pure chitosan is 1.22 % and 1.19 % respectively, while ~1.27% ash

content has been reported in the commercially available chitosan as shown in Figure 3. Comparing the results of moisture, ash content, and solubility it can be stated that the prepared chitosan from shrimp shell was very good quality.

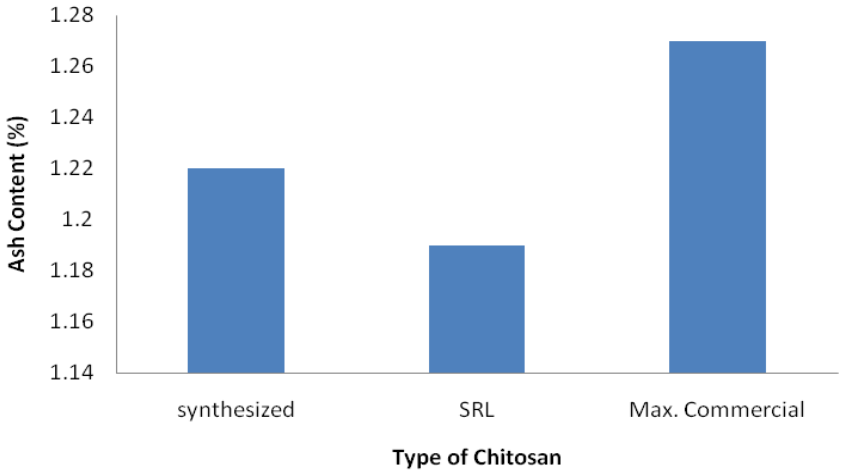

Figure 3: Ash content of the chitosan

Table 1: Moisture, Ash content and Solubility of chitosan.

Obs. No.	Test Parameters	Synthesized (%)	Standard (SRL) (%)	Commercial (%)
1	Moisture	1.25	1.24	1.00 – 1.30
2	Ash	1.22	1.19	~1.27
3	Solubility	Soluble in 1% CH_3COOH	Soluble in 1% CH_3COOH	Soluble in 1% CH_3COOH

3.3 FTIR Spectroscopy

The FTIR spectra of synthesized and reference chitosan are displayed in Figure 4. Standard chitosan is represented by the top spectrum in the illustration, while synthesized chitosan is represented by the lower spectrum. As can be observed from the figure, OH and amine N-H symmetrical stretching vibrations may be the cause of the large absorption band at 3450–3400 cm^{-1}. Symmetric -CH_2- stretching vibration peak at 2950–2800 cm^{-1} were ascribed to the pyranose ring (Pawlak & Mucha, 2003). The structure of saccharide was assigned a peak at 1156 cm^{-1}. In the amide group, the strong peak at 1350 cm^{-1} was attributed to -CH_3 (Zheng et al., 2001). The chitosan's C-O stretching vibration was suggested by the broad peak at 1021 and 1098 cm^{-1}, whereas the amide I and II's -C=O and -NH_2 stretching were responsible for the peaks at 1675 and 1600 cm^{-1}. The anti-symmetric stretching of the C-O-C bridge was attributed to the absorption bands at 1200 cm^{-1}, while the skeletal vibrations related to the C-O stretching were attributed to the bands at 1100 –1020 cm^{-1}. Table 2 also contains a tabulation of the results. As a result, it can be shown that the spectra of extra pure and synthetic chitosan are nearly identical. This outcome unequivocally shows that chitosan was successfully isolated from the leftover shrimp shell.

Table 2: FTIR studies of pure chitosan.

Wave length, (cm^{-1})	Mode & Resolution	Tentative band

3450-3400	symmetric stretching, very broad	-OH and amine N-H
2950-2800	symmetric stretching, broad	-CH_2 (pyranose ring)
1675	symmetric stretching, medium	-C=O (amide I)
1600	symmetric stretching, medium	-NH (amide II)
1350	bending, sharp	-CH_2 in amide group
1200	anti-symmetric stretching	C-O-C bridge
1100-1020	vibrations, broad	-C-O

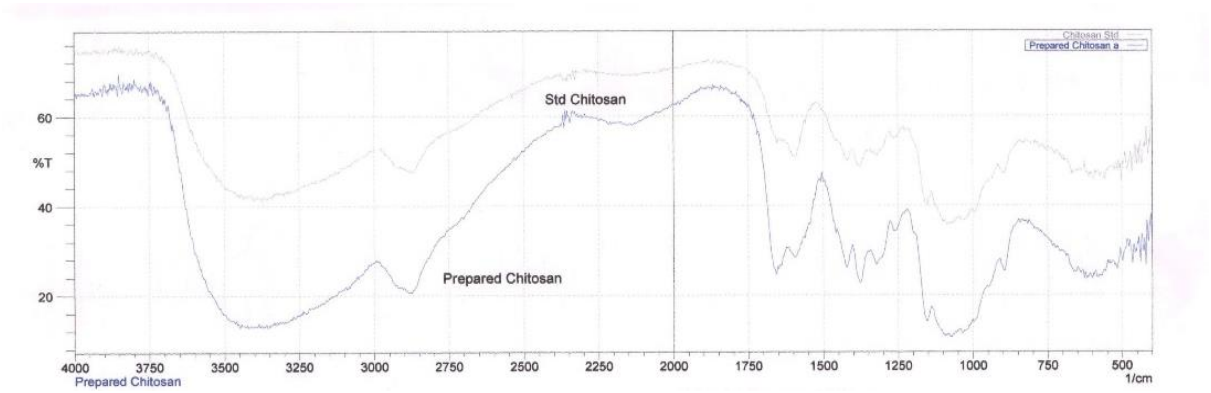

Figure 4: FTIR Spectrum of Prepared and Standard Chitosan

3.3.1 Chitosan Based Metal Nanoparticle

The solution cast process was adapted to synthesize metal nanoparticles based on chitosan. Two distinct nanoparticles (NPs) with varying sizes and shapes were generated are Chi-Zn and Chi-Cu. Every one of the NPs has a distinct type based on the individual raw ingredients that were employed in the synthesis. Figure 5 & Table 3 exhibit the FTIR spectra and data for Chi-Zn NPs and Figure 6 & Table 4 exhibit the FTIR spectra and data for Chi-Zn NPs.

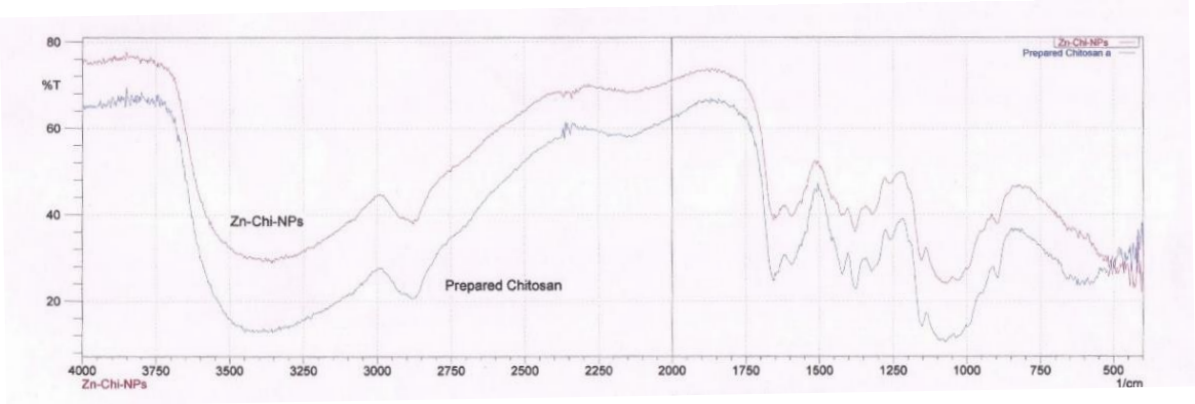

Figure 5: FTIR Spectrum of Prepared Chitosan and Chi-Zn NPs

Table 3: FTIR studies of Chitosan-Zn NPs.

Wave length, (cm^{-1})	Mode & Resolution	Tentative band

3450-3400	symmetric stretching, very broad	-OH and amine N-H
2950-2800	symmetric stretching, broad	-CH_2 (pyranose ring)
1675	symmetric stretching, medium	-C=O (amide I)
1600	symmetric stretching, medium	-NH (amide II)
1350	bending, sharp	-CH_2 in amide group
1200	anti-symmetric stretching	C-O-C bridge
1100-1020	vibrations, broad	-C-O

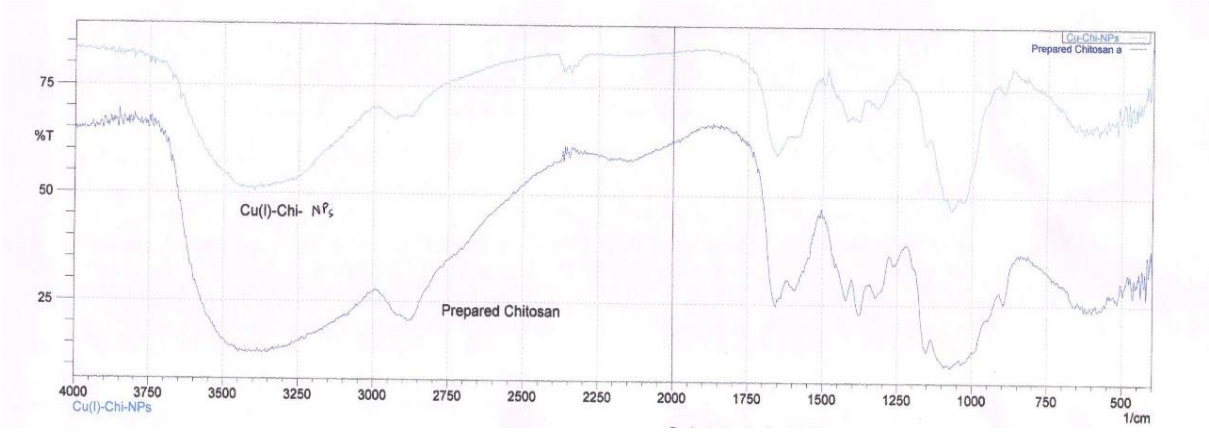

Figure 6: FTIR Spectrum of Prepared Chitosan and Chi-Cu metal NPs

Table 4: FTIR studies of Chi-Cu metal NPs.

Wave length, (cm^{-1})	Mode & Resolution	Tentative band
3450-3400	symmetric stretching, broad	-OH and amine N-H
2950-2800	symmetric stretching, broad	-CH_2 (pyranose ring)
1675	symmetric stretching, medium	-C=O (amide I)
1600	symmetric stretching, medium	-NH (amide II)
1350	bending, sharp	-CH_2 in amide group
1200	anti-symmetric stretching	C-O-C bridge
1100-1020	vibrations, broad	-C-O

3.4 Thermal gravimetric analysis (TGA)

The thermal analyses were obtained by TA Isntruments-2100. Sample in the range of 16-30 mg, but accurately weighted case to case were taken into an aluminum-made crucible of which the volume was 100 µL. Then it was inserted into the furnace. The crucible was hermetically sealed and a pinhole was punched into the crucible lid.

3.4.1 TGA of Chi-Zn NPs

Thermal details of chi-Zn NPs are shown in Table 5 and Figure 7. It can be seen from Figure 7 that three consecutive weight loss steps were observed. The first weight loss was about 6.79 wt% at 55-190 ºC, which might be responsible for the loss of moisture content of adhering water molecules and crystalline water. The second

weight loss was about 25.80 wt% in the range of 220 to 320 ºC, which was due to scission or split of the linkage in the chitosan structure or backbone. In the last and third stage, the loss of weight was about 33.19 wt% in the range of 320-500 ºC, which may be due to the thermal decomposition of glucosamine residues which means the loss of the organic part of the NPs. After that the weight loss could not continued further indicates the presence of metal particles in the Chi-Zn NPs.

Table 5: TGA studies of Chi-Zn NPs

Percentage of Decomposition (%)	Decomposition Temperature (ºC)
10	100
20	270
30	290
40	310
50	430
57	500

Table 6: TGA studies of Chi-Cu NPs

Percentage of Decomposition (%)	Decomposition Temperature (ºC)
10	90
20	180
30	230
40	290
50	350
60	430
70	470
77	500

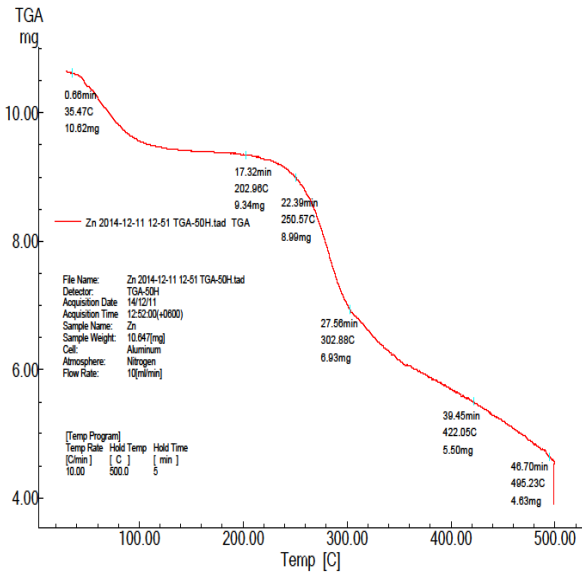

Figure 7: TGA thermogram of Chitosan-Zn NPs

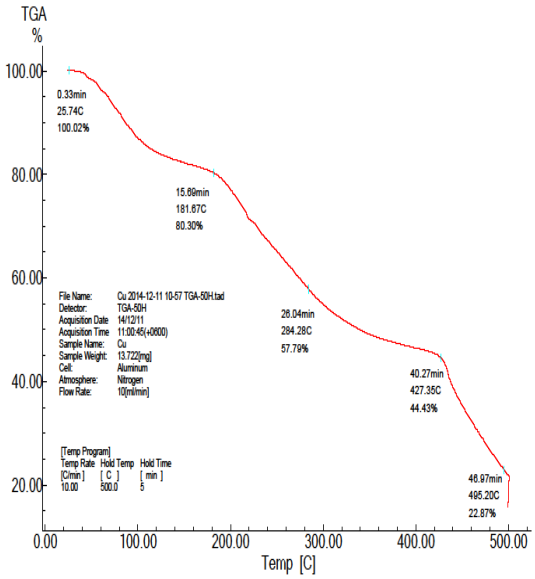

Figure 8: TGA thermogram of Chi-Cu metal NPs.

3.4.2 TGA of Chi-Cu metal NPs

TGA details of chi-Cu(0) NPs are shown in Table 6 and Figure 8. Figure 8 shows that there are also involved three steps for the weight loss of the examined material. The first weight loss was about 19.70 wt% at 40 – 180 ºC, which might be responsible for the loss of moisture content of adhering water molecules and crystalline water. The second weight loss was about 35.87 wt% in the range of 200 to 400 ºC, which was due to the scission of the linkage in the chitosan structure/backbone. In the last or third stage of the range of 420–500 ºC, the weight loss was about 21.57 wt%, which may be due to the thermal decomposition of glucosamine residues which means the loss of organic part of the NPs (Chen et al., 2008). However after that the weight loss could not continued further indicates the presence of metal particles in the Chi-Cu NPs.

3.5 Scanning Electron Microscope analysis

3.5.1 SEM analysis of Chi-Zn NPs

The scanning electron microscope was used to measure the size and shape of the nanoparticles. The SEM image was captured with magnifications of X5,000 and X10,000. Figure 9 shows the photographs of Chi-Zn nanoparticles. The figure demonstrates that the majority of Chi-Zn NPs morphologies have smooth surfaces and flakes-like shapes, with particle sizes ranging from 10 to 50 nm. These findings were in reasonable agreement with those of Radyum Ikono (2012) (Ikono et al., 2012) and Saptashi Ghosh (2014) (Ghosh et al., 2014).

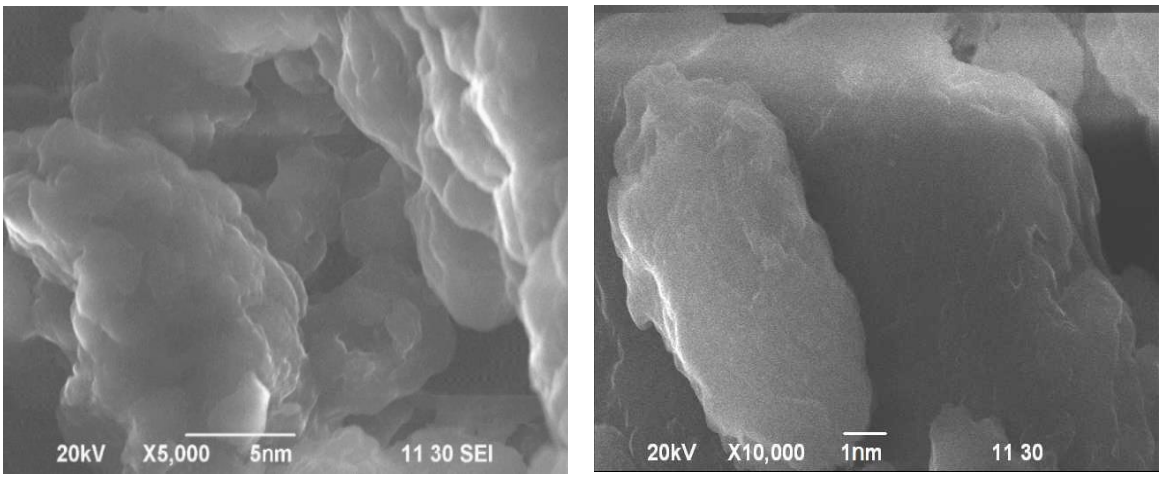

Figure 9: SEM of Chitosan-Zn NPs

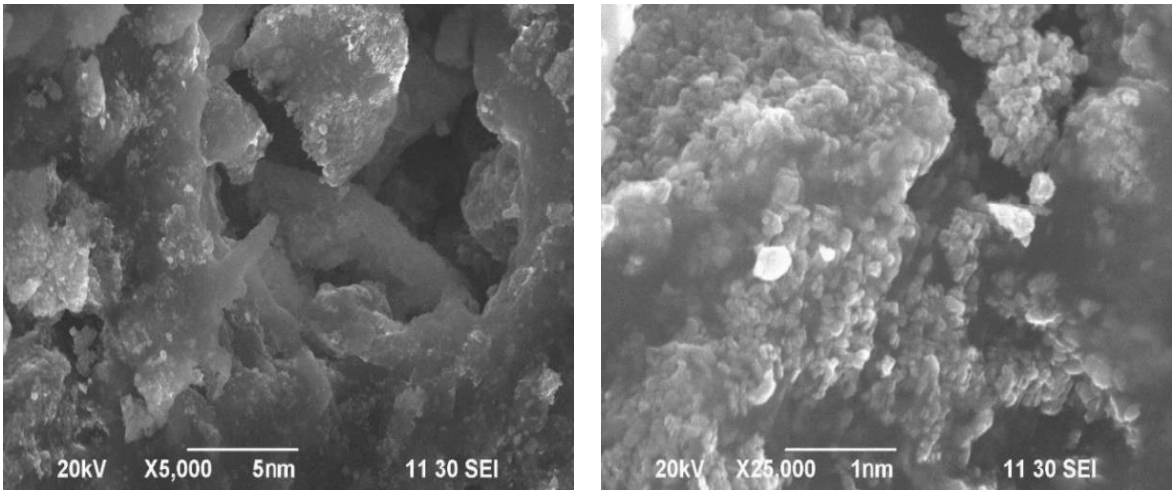

Figure 10: SEM of Chitosan-Cu NPs

3.5.2 SEM analysis of Chi-Cu metal NPs

Chi-Cu metal NPs were imaged using a SEM at X5,000 and X25,000 magnifications. As seen by the nanoparticle photos in Figure 10, the majority of Chi-Cu metal NPs morphologies are likewise flakes-like, similar to Chi-Zn NPs. The particles ranged in size from 10 to 50 nm, and the surface was not smooth.

3.6 Antibacterial Analysis

The antibacterial properties of the targeted chitosan-metal NPs against four Gram-negative bacteria were observed in biological assessments. The results of the target compounds' antibacterial activity on agar disc diffusion tests

are shown in Table 7 and depicted in Figures 11 and 12 respectively. The standard drug kanamycin's zone of inhibition (measured in millimeters) against the Gram-negative bacteria *Pseudomonas aeruginosa*, *Salmonella bovismorbificans*, *Salmonella typhi* and *Escherichia coli* were found 22 mm, 22 mm, 20 mm and 20 mm respectively. Figure 13 displays a graphical comparison of the zone of inhibition between the microorganisms and the chitosan-metal nanoparticles. Under identical circumstances, Table 7 demonstrates that Chi-Cu NPs have 32 mm, 36 mm, 37 mm, and 32 mm against *Pseudomonas aeruginosa*, *Salmonella bovis-morbificans*, *Salmonella typhi* and *Escherichia coli* respectively, while Chi-Zn NPs has 38 mm, 31 mm, 30 mm and 39 mm respectively. Conversely, according to literature, the chitosan's zone of inhibition for Escherichia coli 19 mm (Soleimani et al., 2015), while it is 12 mm (Soleimani et al., 2015) for Pseudomonas aeruginosa. We discovered from this antibacterial activity assay that both of the produced NPs are very active. All of the complexes are even more potent than kanamycin, the prescribed medication. Chi-Zn NPs demonstrated the highest inhibitory zones for all four complexes, while against *Pseudomonas aeruginosa* and *Escherichia coli* bacteria, almost twice as much as the antibiotic kanamycin. Chi-Cu metal NPs have the maximum inhibition zone in case of *Salmonella bovismorbificans* and *Salmonella typhi*.

Table 7: Results of the antibacterial activity of the different NPs

Bacteria code	Name of the bacteria	Diameter of inhibition zone of bacteria in different NPs (mm)		
		Chi-Zn NPs	Chi-Cu NPs	Kanamycin 30µg/disc
A	*Psudomonas aeruginosa* (-ve)	38	32	22
B	*Salmonella bovis morbificans*(-ve)	31	36	22
C	*Salmonella typhi* (-ve)	30	37	20
D	*Escherichia coli* (-ve)	39	32	20

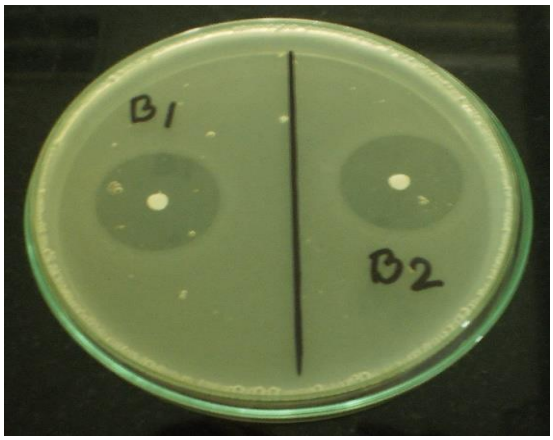

Figure 11: Photographic representation of zone of inhibition of NPs **1** and **2** respectively against the bacteria *Salmonella bovis morbificans.*

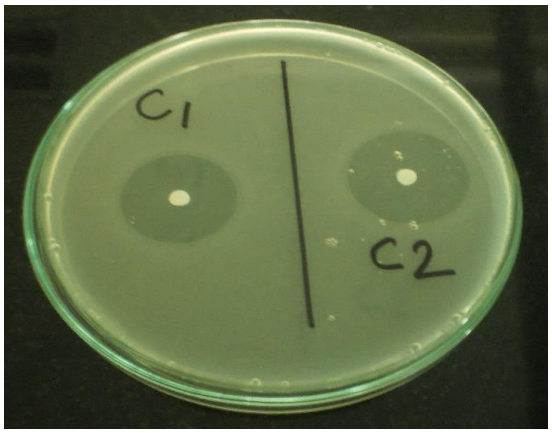

Figure 12: Photographic representation of zone of inhibition of NPs **1** and **2** respectively against the bacteria *Salmonella typhi.*

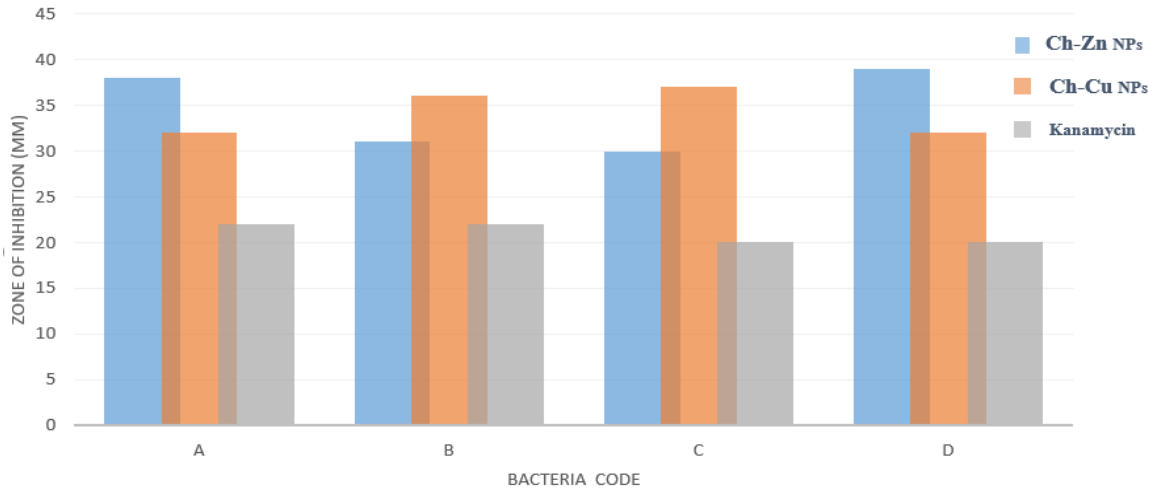

Figure 13: Graphical comparison of zone of inhibition of the NPs 1 and 2 with standard (Kanamycin)

4. CONCLUSION

Our attempts to produce chitosan from shrimp shells and chitosan-metal NPs have been successful. Prepared NPs exhibit greater antibacterial activity than the widely used drug kanamycin. Chi-Zn NPs demonstrated the strongest inhibitory zones of all four bacteria, while against *Pseudomonas aeruginosa* and *Escherichia coli bacteria*, almost twice as much as the conventional antibiotic kanamycin. When it comes to Salmonella typhi and Salmonella bovismorbificans, Chi-Cu metal NPs have the largest inhibitory zone. We believe that our green time saving, environmentally friendly and economically viable technique will play a great role in the synthesis of chitosan nanoparticles and prepared NPs could be applied as an antibacterial agent/drug.

ACKNOWLEDGEMENTS

We gratefully acknowledge UGC for research grants; Khulna University of Engineering & Technology, Khulna, Bangladesh; ACI Pharmaceuticals Ltd. Bangladesh and the Department of Fisheries, Fish Inspection & Quality Control microbiological laboratory in Khulna, Bangladesh for the facilities given to conduct the research.

REFERENCES

AbdElhady, M. (2012). Preparation and characterization of chitosan/zinc oxide nanoparticles for imparting antimicrobial and UV protection to cotton fabric. *International journal of carbohydrate chemistry*, *2012*(1), 840591.

Ahmed, F., Mustafa, M. A., Tayyab, M., Sarwer, M. U., Khan, H. U., & Zaheer, L. (2023). Fabrication and In vitro Evaluation of Chitosan-based Nanocomposites through Ionic Gelation Method for the Sustained Release Drug Delivery of Nicorandil. *Asian Journal of Pharmaceutical Research and Health Care*, *15*(4), 338-346.

Ahmed, S. B., Mohamed, H. I., Al-Subaie, A. M., Al-Ohali, A. I., & Mahmoud, N. M. (2021). Investigation of the antimicrobial activity and hematological pattern of nano-chitosan and its nano-copper composite. *Scientific Reports*, *11*(1), 9540.

Al-Jumaili, B. E. B., Talib, Z. A., Zakaria, A., Ramizy, A., Ahmed, N. M., Paiman, S. B., Ying, J. L., Muhd, I. B., & Baqiah, H. (2018). Impact of ablation time on Cu oxide nanoparticle green synthesis via pulsed laser ablation in liquid media. *Applied Physics A*, *124*, 1-6.

Ates, B., Koytepe, S., Ulu, A., Gurses, C., & Thakur, V. K. (2020). Chemistry, structures, and advanced applications of nanocomposites from biorenewable resources. *Chemical reviews*, *120*(17), 9304-9362.

Ba-Abbad, M. M., Kadhum, A. A. H., Mohamad, A. B., Takriff, M. S., & Sopian, K. (2013). The effect of process parameters on the size of ZnO nanoparticles synthesized via the sol–gel technique. *Journal of Alloys and Compounds*, *550*, 63-70.

Banitaba, S. N., Ebadi, S. V., Salimi, P., Bagheri, A., Gupta, A., Arifeen, W. U., Chaudhary, V., Mishra, Y. K., Kaushik, A., & Mostafavi, E. (2022). Biopolymer-based electrospun fibers in electrochemical devices: versatile platform for energy, environment, and health monitoring. *Materials Horizons*, *9*(12), 2914-2948.

Benchasattabuse, D. (2015). Microencapsulation of virgin coconut oil in β-cyclodextrin by using paste method.

Bhosale, M. A., & Bhanage, B. M. (2016). A simple approach for sonochemical synthesis of Cu2O nanoparticles with high catalytic properties. *Advanced Powder Technology*, *27*(1), 238-244.

Borges, A., Ferreira, C., Saavedra, M. J., & Simões, M. (2013). Antibacterial activity and mode of action of ferulic and gallic acids against pathogenic bacteria. *Microbial Drug Resistance*, *19*(4), 256-265.

Chan, H.-K., & Kwok, P. C. L. (2011). Production methods for nanodrug particles using the bottom-up approach. *Advanced drug delivery reviews*, *63*(6), 406-416.

Chen, C.-H., Wang, F.-Y., Mao, C.-F., Liao, W.-T., & Hsieh, C.-D. (2008). Studies of chitosan: II. Preparation and characterization of chitosan/poly (vinyl alcohol)/gelatin ternary blend films. *International journal of biological macromolecules*, *43*(1), 37-42.

Cioffi, N., Torsi, L., Ditaranto, N., Tantillo, G., Ghibelli, L., Sabbatini, L., Bleve-Zacheo, T., D'Alessio, M., Zambonin, P. G., & Traversa, E. (2005). Copper nanoparticle/polymer composites with antifungal and bacteriostatic properties. *Chemistry of Materials*, *17*(21), 5255-5262.

Corbalán, N., Quiroga, M., Masias, E., Peralta, D., Velázquez, J. B., Acuña, L., & Vincent, P. (2021). Antimicrobial activity of MccJ25 (G12Y) against gram-negative foodborne pathogens in vitro and in food models. *International Journal of Food Microbiology*, *352*, 109267.

Detsi, A., Kavetsou, E., Kostopoulou, I., Pitterou, I., Pontillo, A. R. N., Tzani, A., Christodoulou, P., Siliachli, A., & Zoumpoulakis, P. (2020). Nanosystems for the encapsulation of natural products: The case of chitosan biopolymer as a matrix. *Pharmaceutics*, *12*(7), 669.

Esteban-Cubillo, A., Pecharromán, C., Aguilar, E., Santarén, J., & Moya, J. S. (2006). Antibacterial activity of copper monodispersed nanoparticles into sepiolite. *Journal of Materials Science*, *41*, 5208-5212.

Gerbreders, V., Krasovska, M., Sledevskis, E., Gerbreders, A., Mihailova, I., Tamanis, E., & Ogurcovs, A. (2020). Hydrothermal synthesis of ZnO nanostructures with controllable morphology change. *CrystEngComm*, *22*(8), 1346-1358.

Ghosh, S., Majumder, D., Sen, A., & Roy, S. (2014). Facile sonochemical synthesis of zinc oxide nanoflakes at room temperature. *Materials Letters*, *130*, 215-217.

Ikono, R., Akwalia, P. R., Siswanto, W. B. W., Sukarto, A., & Rochman, N. T. (2012). Effect of PH variation on particle size and purity of nano zinc oxide synthesized by sol-gel method. *Int J Engl Technol*, *12*, 5-9.

Karki, S., Gohain, M. B., Yadav, D., & Ingole, P. G. (2021). Nanocomposite and bio-nanocomposite polymeric materials/membranes development in energy and medical sector: A review. *International journal of biological macromolecules*, *193*, 2121-2139.

Khan, A., & Alamry, K. A. (2021). Recent advances of emerging green chitosan-based biomaterials with potential biomedical applications: A review. *Carbohydrate Research*, *506*, 108368.

Khan, A., Rashid, A., Younas, R., & Chong, R. (2016). A chemical reduction approach to the synthesis of copper nanoparticles. *International Nano Letters*, *6*, 21-26.

Khan, M. A., Nayan, N., Ahmad, M. K., Fhong, S. C., Ali, M. S. M., Mustafa, M. K., & Tahir, M. (2021). Interface study of hybrid CuO nanoparticles embedded ZnO nanowires heterojunction synthesized by controlled vapor deposition approach for optoelectronic devices. *Optical Materials*, *117*, 111132.

Lefnaoui, S., Rebouh, S., Bouhedda, M., Yahoum, M. M., & Hanini, S. (2018). Artificial neural network modeling of sustained antihypertensive drug delivery using polyelectrolyte complex based on carboxymethyl-kappa-carrageenan and chitosan as prospective carriers. 2018 International conference on applied smart systems (ICASS),

Mallick, S., Sharma, S., Banerjee, M., Ghosh, S. S., Chattopadhyay, A., & Paul, A. (2012). Iodine-stabilized Cu nanoparticle chitosan composite for antibacterial applications. *ACS applied materials & interfaces*, *4*(3), 1313-1323.

O'neill, J. (2014). Antimicrobial resistance: tackling a crisis for the health and wealth of nations. *Rev. Antimicrob. Resist.*

Ohya, Y., Shiratani, M., Kobayashi, H., & Ouchi, T. (1994). Release behavior of 5-fluorouracil from chitosan-gel nanospheres immobilizing 5-fluorouracil coated with polysaccharides and their cell specific cytotoxicity. *Journal of Macromolecular Science—Pure and Applied Chemistry*, *31*(5), 629-642.

Park, B. K., Jeong, S., Kim, D., Moon, J., Lim, S., & Kim, J. S. (2007). Synthesis and size control of monodisperse copper nanoparticles by polyol method. *Journal of colloid and interface science*, *311*(2), 417-424.

Pawlak, A., & Mucha, M. (2003). Thermogravimetric and FTIR studies of chitosan blends. *Thermochimica acta*, *396*(1-2), 153-166.

Qiu, S., Dong, J., & Chen, G. (1999). Preparation of Cu nanoparticles from water-in-oil microemulsions. *Journal of colloid and interface science*, *216*(2), 230-234.

Raoufi, D. (2013). Synthesis and microstructural properties of ZnO nanoparticles prepared by precipitation method. *Renewable Energy*, *50*, 932-937.

Rosales-Martínez, P., Cornejo-Mazón, M., Arroyo-Maya, I. J., & Hernández-Sánchez, H. (2018). Chitosan micro- and nanoparticles for vitamin encapsulation. In *Nanotechnology applications in the food industry* (pp. 427-440). CRC Press.

Salavati-Niasari, M., & Davar, F. (2009). Synthesis of copper and copper (I) oxide nanoparticles by thermal decomposition of a new precursor. *Materials Letters*, *63*(3-4), 441-443.

Soleimani, N., Mobarez, A. M., Olia, M. S. J., & Atyabi, F. (2015). Synthesis, characterization and effect of the antibacterial activity of chitosan nanoparticles on vancomycin-resistant Enterococcus and other gram negative or gram positive bacteria. *International Journal of Pure and Applied Sciences and Technology*, *26*(1), 14.

Soomro, R. A., Sherazi, S. H., Memon, N., Shah, M., Kalwar, N., Hallam, K. R., & Shah, A. (2014). Synthesis of air stable copper nanoparticles and their use in catalysis. *Adv. Mater. Lett*, *5*(4), 191-198.

Tanwar, J., Das, S., Fatima, Z., & Hameed, S. (2014). Multidrug resistance: an emerging crisis. *Interdisciplinary perspectives on infectious diseases*, *2014*(1), 541340.

Tito, I. A., UddIN, M. S., ISLAM, M. S., & Bhowmik, S. (2021). Copper Nanoparticle (CuNP's) Synthesis by the Various Ways with Photocatalytic and Antibacterial Activity (A-Review). *Oriental Journal of Chemistry*, *37*(5).

Torres, F. G., Troncoso, O. P., Pisani, A., Gatto, F., & Bardi, G. (2019). Natural polysaccharide nanomaterials: an overview of their immunological properties. *International journal of molecular sciences*, *20*(20), 5092.

Verma, S., Gokhale, R., & Burgess, D. J. (2009). A comparative study of top-down and bottom-up approaches for the preparation of micro/nanosuspensions. *International journal of pharmaceutics*, *380*(1-2), 216-222.

Victor, S. P., Paul, W., & Sharma, C. P. (2013). Chitosan self-aggregates and micelles in drug delivery. *J. Nanopharm. Drug Delivery*, *1*, 193.

Vivas, R., Barbosa, A. A. T., Dolabela, S. S., & Jain, S. (2019). Multidrug-resistant bacteria and alternative methods to control them: an overview. *Microbial Drug Resistance*, *25*(6), 890-908.

Wallace, R., Brown, A., Brydson, R., Wegner, K., & Milne, S. (2013). Synthesis of ZnO nanoparticles by flame spray pyrolysis and characterisation protocol. *Journal of Materials Science*, *48*, 6393-6403.

Wang, L., & Muhammed, M. (1999). Synthesis of zinc oxide nanoparticles with controlled morphology. *Journal of Materials Chemistry*, *9*(11), 2871-2878.

Wang, X., Du, Y., & Liu, H. (2004). Preparation, characterization and antimicrobial activity of chitosan–Zn complex. *Carbohydrate polymers*, *56*(1), 21-26.

Ye, L., Cao, Z., Liu, X., Cui, Z., Li, Z., Liang, Y., Zhu, S., & Wu, S. (2022). Noble metal-based nanomaterials as antibacterial agents. *Journal of Alloys and Compounds*, *904*, 164091.

Zangeneh, M. M., Ghaneialvar, H., Akbaribazm, M., Ghanimatdan, M., Abbasi, N., Goorani, S., Pirabbasi, E., & Zangeneh, A. (2019). Novel synthesis of Falcaria vulgaris leaf extract conjugated copper nanoparticles with potent cytotoxicity, antioxidant, antifungal, antibacterial, and cutaneous wound healing activities under in vitro and in vivo condition. *Journal of Photochemistry and Photobiology B: Biology*, *197*, 111556.

Zheng, H., Du, Y., Yu, J., Huang, R., & Zhang, L. (2001). Preparation and characterization of chitosan/poly (vinyl alcohol) blend fibers. *Journal of Applied Polymer Science*, *80*(13), 2558-2565.